ChemBioChem

Supporting Information

Ratiometric Detection of Glutathione Based on Disulfide Linkage Rupture between a FRET Coumarin Donor and a Rhodamine Acceptor

Yibin Zhang,* Shuai Xia, Shulin Wan, Tessa E. Steenwinkel, Tara Vohs, Rudy L. Luck,* Thomas Werner,* and Haiying Liu*

Contents

1. Summary of some reported fluroescent probes

Chemical structure of reported probe	Reactivity (Time)	Sensitivity (LOD)	Water solubility	Cells for imaging	Reference
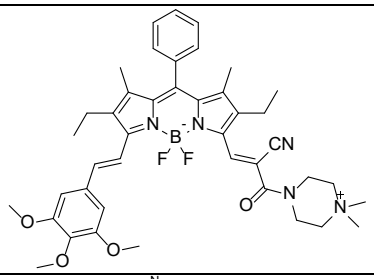		3.4 μM	PIPES buffer (50 mM, 100 mM KCl, pH 7.4)	A549 cells	1
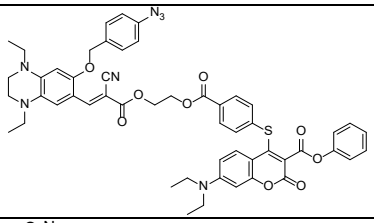	30 min	0.012 μM	HEPES bufferat	HeLa cells	2
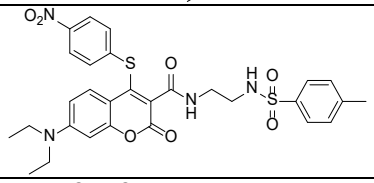	38 min	23 nM	PBS buffer	HeLa cells	3
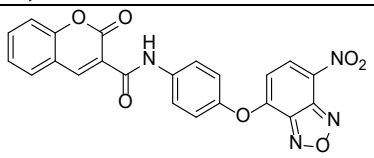	10 min	0.36 μM	PBS buffer	HeLa cells	4
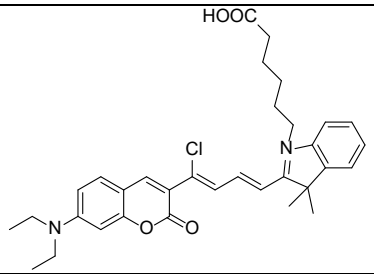	120 min	2.596 μM	PBS buffer	A375 cells.	5
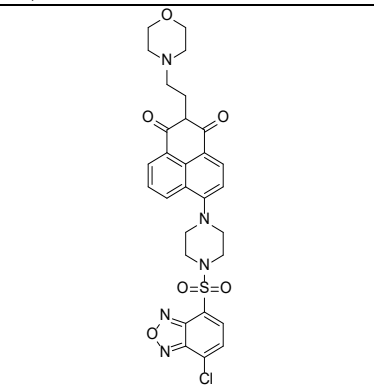	60 min	0.54 μM	PBS buffer	HeLa cells	6

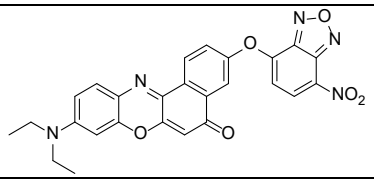	30 min	0.11 μM	PBS buffer	HeLa cells	7
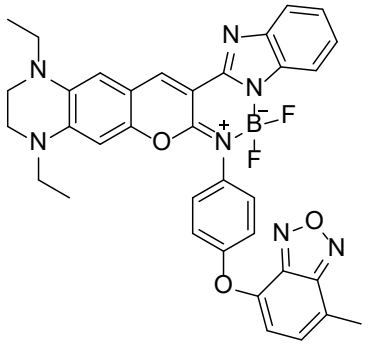	8 min	39.3 nM	PBS buffer	HeLa cells	8
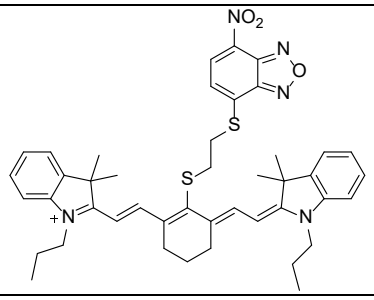		75 nM	PBS buffer	U87 cells	9
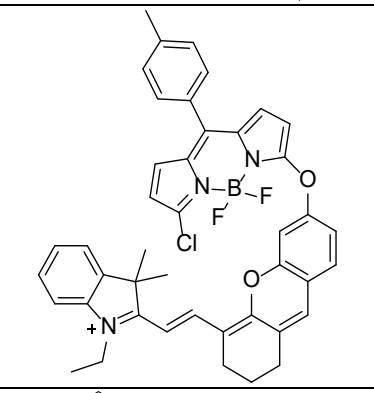		1.37 μM	PBS buffer	HepG-2 cells	10
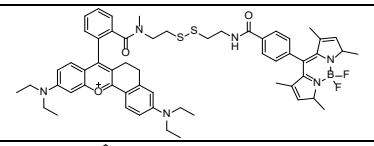	90 min	0.26 μM	PBS buffer	HeLa cells	11
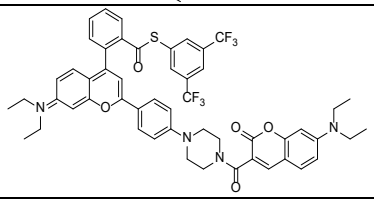	40 min		PBS buffer	HeLa cells	12

2. Instrumentation

400 MHz Inova NMR spectrometer was employed to record ^{1}H NMR spectra at 400 NHz, and ^{13}C NMR spectra at 100 MHz. Chemical shifts (δ) of intermediates and probes were determined by using internal standards in ppm from solvent residual peaks (^{1}H: δ 7.26 for $CDCl_3$, δ 2.50 for DMSO-d_6; ^{13}C: δ 77.3 for $CDCl_3$). High-resolution mass spectra were recorded either on a Fast atom bombardment (FAB) ionization mass spectrometer or a matrix assisted laser desorption/ionization time of flight mass spectrometer. Absorption spectra were carried out using a Perkin Elmer Lambda 35 UV/VIS spectrometer while fluorescence spectra were obtained by using a Jobin Yvon Fluoromax-4 spectrofluorometer with a 420 nm cut-off filter to remove radiation source below 420 nm. A Zeiss LSM510 confocal microscope and an Olympus IX71 inverted microscope (side-port 808nm laser) were used for cellular imaging.

3. Determination of probe fluorescence quantum yields

All absorbance spectra and emission spectra were obtained at room temperature using a standard 1 cm path length quartz fluorescence cuvette. The slit widths of excitation and emission of fluorescence measurements were both set to 5 nm. Fluorescence quantum yields were calculated by measuring fluorescence of fluorophores of known quantum yield with the same experimental parameters (excitation wavelength and slit width) [13]. The samples and the reference solutions were freshly prepared under identical conditions. The fluorescence quantum yields were calculated using the following equation [14]:

$$\Phi_X = \Phi_{st}(Grad_X/Grad_{st})(\eta_X^2/\eta_{st}^2)$$

where the subscripts '*st*' and '*X*' stand for standard and test, respectively, Φ is the fluorescence quantum yield, "*Grad*" represents the gradient from the plot of integrated fluorescence intensity versus absorbance and η is the refractive index of the solvent.

Rhodamine 6G (0.95 in ethanol) [15] was used as standard to calculate the quantum yield of the coumarin moiety, and a near-infrared rhodamine dye (0.37 in pH 7.4 PBS buffer with 10% ethanol) [16] below was utilized as a reference standard to calculate the fluorescence quantum yields of the rhodamine moiety in ethanol and buffer solutions. The absorbance was kept between 0.05 and 0.1 to obtain optimized data. All the samples and references were freshly prepared under identical conditions.

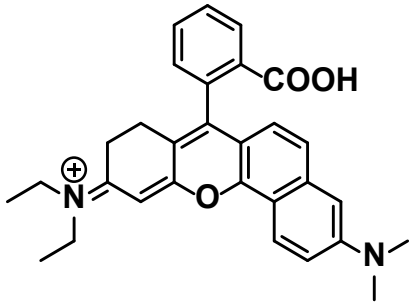

Near-infrared rhodamine dye as the fluorescence standard

4. Theoretical calculation

Data for the Glutathione Probe A

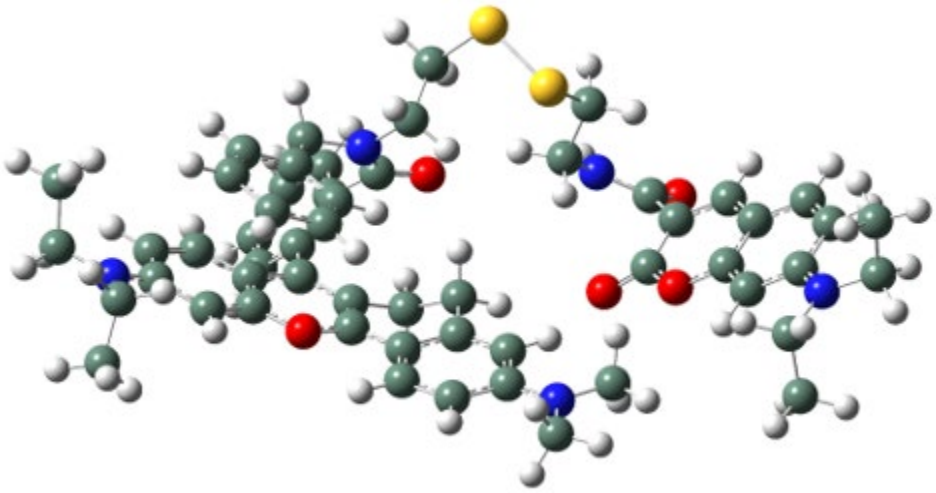

Figure S1. GaussView representation of probe **A**.

Table S1. Calculated atomic coordinates for probe **A**.

Row	Symbol	X	Y	Z	Row	Symbol	X	Y	Z
1	C	-7.07542	0.38269	0.209092	42	N	2.851201	-3.83311	0.880863
2	C	-6.83822	1.766348	-0.07668	43	C	-3.7396	-0.36234	-1.85311
3	C	-5.59392	2.308485	0.312795	44	C	4.096767	-3.66262	1.377139
4	C	-4.63751	1.486233	0.862517	45	O	4.651291	-4.52323	2.072464
5	C	-4.84076	0.11231	1.131553	46	C	4.816967	-2.39827	1.032196
6	C	-6.11357	-0.40349	0.785859	47	C	4.279507	-1.11862	1.436591
7	O	-3.42652	2.054648	1.103006	48	O	5.01242	0.002884	1.107248
8	C	-2.38653	1.327443	1.525655	49	C	6.205905	-0.05398	0.447141
9	C	-2.53327	-0.0253	1.876189	50	C	6.76961	-1.29927	0.09934
10	C	-3.76021	-0.64211	1.654398	51	C	6.042156	-2.46664	0.42321
11	C	-1.13601	2.004916	1.560638	52	C	6.817215	1.149843	0.163491
12	C	0.053019	1.2377	1.700519	53	C	8.063215	1.168136	-0.50849
13	C	-0.05347	-0.25838	1.822478	54	C	8.647687	-0.09007	-0.86024
14	C	-1.3397	-0.66304	2.534609	55	C	8.016015	-1.2739	-0.56302
15	C	-3.96122	-2.08355	1.921952	56	N	8.678007	2.340406	-0.80931
16	C	-3.26415	-3.07134	1.206931	57	C	10.0072	2.390493	-1.40635
17	C	-3.52469	-4.42159	1.465431	58	C	8.037299	3.626585	-0.56364
18	C	-4.47076	-4.79618	2.414807	59	O	3.244787	-0.93079	2.058823
19	C	-5.15133	-3.81662	3.13923	60	C	-2.73247	0.563577	-1.57313
20	C	-4.8972	-2.47154	2.89002	61	C	-2.85909	1.894958	-1.97224
21	N	-7.75699	2.513496	-0.73124	62	C	-3.99965	2.316906	-2.65204
22	C	-7.46713	3.877096	-1.15954	63	C	-5.01498	1.398154	-2.93016
23	C	-7.79122	4.914493	-0.08811	64	C	-4.88226	0.068928	-2.53715
24	C	-9.03166	1.263313	-2.458	65	C	-3.64872	-1.82163	-1.45692
25	C	-9.06197	1.984907	-1.11325	66	C	9.97515	2.332984	-2.93152
26	C	-2.13054	-2.80393	0.255426	67	C	8.285697	4.157384	0.846398
27	O	-1.00391	-3.19445	0.588057	68	H	-8.01627	-0.07546	-0.06897
28	N	-2.34825	-2.21535	-0.94468	69	H	-5.33268	3.343417	0.136582
29	C	-1.02992	3.400344	1.367478	70	H	-6.32336	-1.45393	0.95967
30	C	0.194412	4.022526	1.333751	71	H	-0.04483	-0.69893	0.815249
31	C	1.396812	3.266442	1.475595	72	H	0.823626	-0.66021	2.334591
32	C	1.283681	1.858844	1.651875	73	H	-1.30314	-0.314	3.577259
33	N	2.607296	3.870117	1.441651	74	H	-1.43565	-1.74839	2.564951
34	C	3.820895	3.077022	1.520026	75	H	-2.97336	-5.17836	0.914451
35	C	2.71682	5.307715	1.264109	76	H	-4.66772	-5.84902	2.596001
36	C	-1.2211	-2.15546	-1.87384	77	H	-5.87902	-4.09814	3.895052
37	C	-0.85476	-3.53342	-2.41318	78	H	-5.42154	-1.70287	3.451356
38	S	0.516631	-3.51193	-3.62793	79	H	-6.42011	3.939801	-1.47079
39	S	1.990076	-2.30715	-2.82618	80	H	-8.05921	4.064934	-2.06039
40	C	2.795967	-3.3227	-1.53807	81	H	-7.56921	5.92155	-0.45518
41	C	2.20887	-3.0402	-0.15437	82	H	-8.8518	4.876139	0.180556

Row	Symbol	X	Y	Z	Row	Symbol	X	Y	Z
83	H	-7.2059	4.744755	0.820802	106	H	2.429511	-4.72307	1.116509
84	H	-10.0302	0.896616	-2.71616	107	H	6.456673	-3.43967	0.167352
85	H	-8.70138	1.937889	-3.25448	108	H	6.329937	2.059774	0.484788
86	H	-8.34799	0.409219	-2.43349	109	H	9.593132	-0.1232	-1.38731
87	H	-9.43694	1.331793	-0.32063	110	H	8.475805	-2.21611	-0.85014
88	H	-9.75225	2.833048	-1.15084	111	H	10.47453	3.322281	-1.07238
89	H	-1.93245	3.992475	1.2504	112	H	10.62152	1.585376	-0.99317
90	H	0.233254	5.095881	1.192388	113	H	8.42934	4.329448	-1.30542
91	H	2.168048	1.237713	1.749585	114	H	6.965699	3.541717	-0.77028
92	H	3.875138	2.353972	0.699743	115	H	-1.84483	0.253347	-1.03016
93	H	4.681126	3.741876	1.457865	116	H	-2.06794	2.601936	-1.73579
94	H	3.880303	2.526185	2.465046	117	H	-4.10201	3.354747	-2.95841
95	H	2.185278	5.846511	2.055915	118	H	-5.91489	1.719651	-3.44799
96	H	3.767002	5.590567	1.310456	119	H	-5.67552	-0.64264	-2.75671
97	H	2.318303	5.625116	0.293167	120	H	-4.40476	-2.05429	-0.70266
98	H	-1.49354	-1.48866	-2.69406	121	H	-3.88706	-2.44454	-2.32956
99	H	-0.36046	-1.71691	-1.36198	122	H	10.98997	2.396641	-3.33721
100	H	-0.606	-4.21443	-1.59677	123	H	9.523057	1.400771	-3.28397
101	H	-1.68517	-3.9641	-2.98402	124	H	9.393219	3.165667	-3.33981
102	H	2.705737	-4.37892	-1.81101	125	H	7.797864	5.128499	0.978656
103	H	3.856609	-3.05125	-1.57049	126	H	7.895202	3.47295	1.605705
104	H	2.299512	-1.97918	0.088178	127	H	9.357296	4.287425	1.028893
105	H	1.142602	-3.27303	-0.1254					

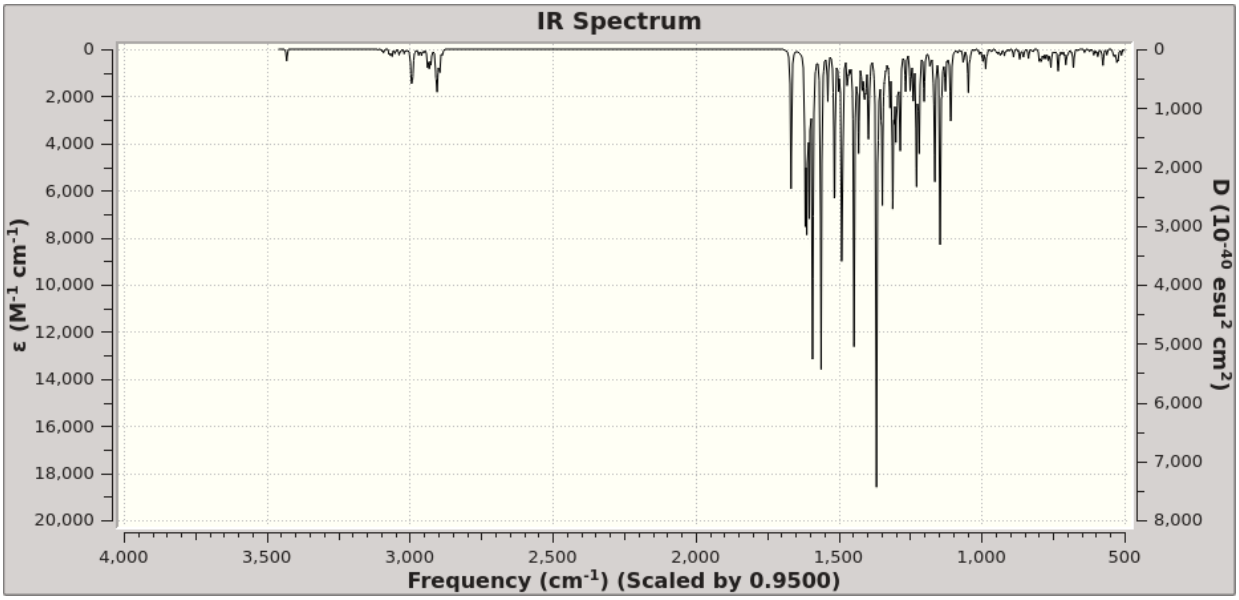

Figure S2. Calculated IR spectrum for probe **A**.

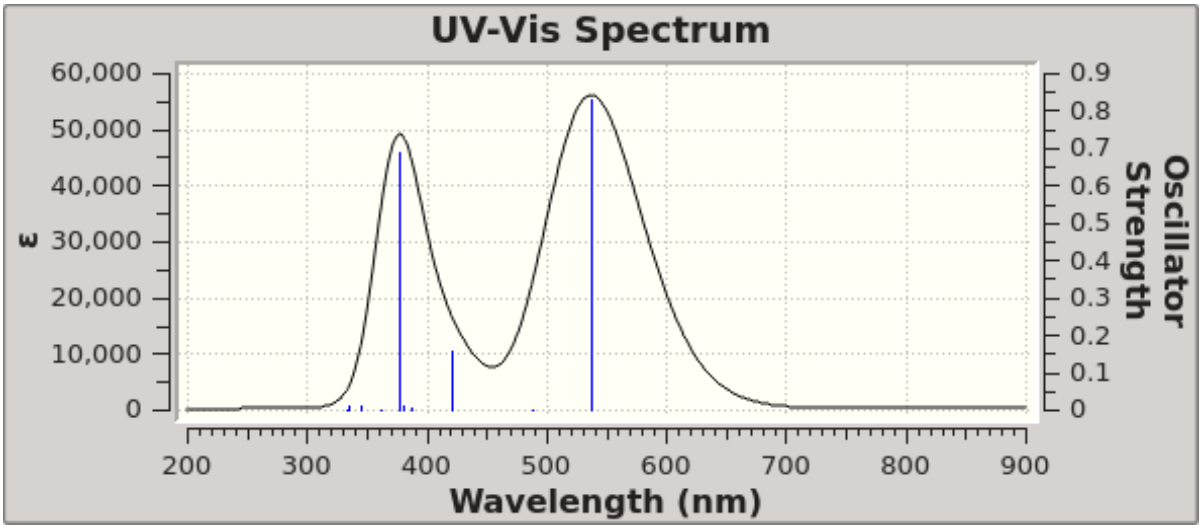

Figure S3. Calculated UV-Vis spectrum for probe **A**.

Table S2. Excitation energies and oscillator strengths listing for Probe **A**.

Excited State	**Nature**	**E (eV)**	**λ(nm)**	***f***	**Orbital transitions**	**Normalized coefficient**
1:	A	2.3062	537.62	0.8280	248 -> 249	0.70104
2:	A	2.5400	488.12	0.0001	247 -> 249	0.70667
3:	A	2.9483	420.53	0.1576	246 -> 249	0.68419
4:	A	3.2058	386.75	0.0041	248 -> 250	0.69927
5:	A	3.2520	381.25	0.0097	244 -> 249	-0.14485
					245 -> 249	0.68249
6:	A	3.2930	376.50	0.6879	247 -> 250	0.69836
7:	A	3.4244	362.06	0.0002	243 -> 249	-0.28382
					244 -> 249	0.61799
					245 -> 249	0.16062
8:	A	3.5907	345.29	0.0111	241 -> 249	0.66556
					243 -> 249	-0.20804
9:	A	3.7043	334.70	0.0083	240 -> 249	0.48630
					241 -> 249	-0.18954
					243 -> 249	-0.40937
					244 -> 249	-0.20961
10:	A	3.7142	333.81	0.0013	239 -> 249	0.37814
					240 -> 249	0.42783
					241 -> 249	0.10634
					243 -> 249	0.34219
					244 -> 249	0.15859

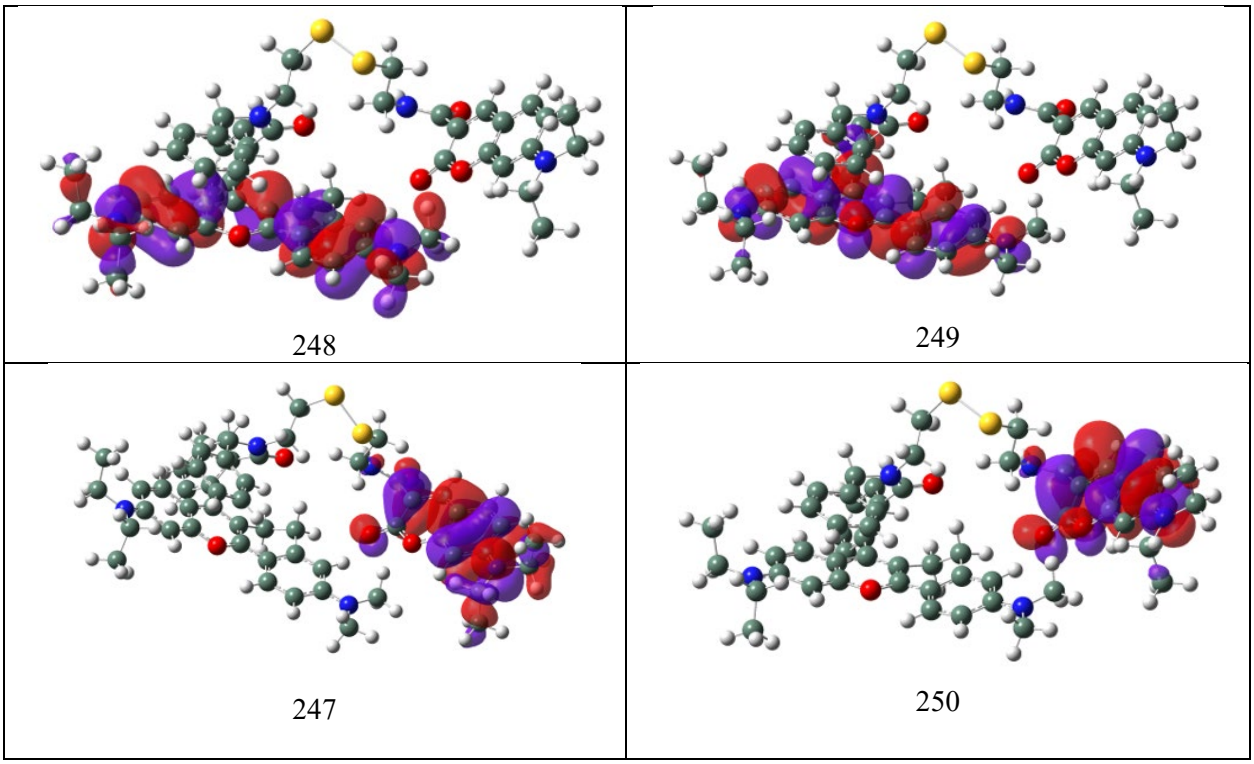

Figure S4. GaussView[17] drawings of orbitals pertaining to Excited State 1 (248, 249) and 6 (247,250), see Table S2.

Data for **B**.

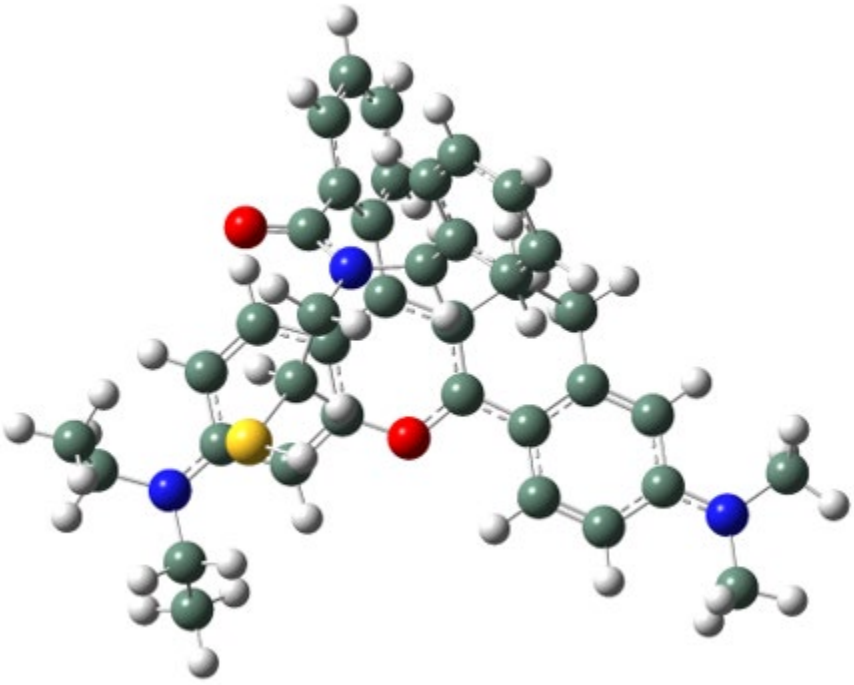

Figure S5. GaussView representation of N-(7-(2-(benzyl(2-mercaptoethyl)carbamoyl)phenyl)-3-(dimethylamino)-5,6-dihydro-10H-benzo[c]xanthen-10-ylidene)-N-ethylethanaminium, **B**.

Table S3. Calculated atomic coordinates for Probe **B**.

Row	Symbol	X	Y	Z	Row	Symbol	X	Y	Z
1	C	0.625056	2.999177	4.38781	18	C	3.415573	-1.60302	1.307396
2	C	0.235237	1.830731	3.746446	19	C	2.978434	-2.66602	0.454001
3	C	0.671717	1.547563	2.449255	20	C	1.591699	-2.77094	0.20801
4	C	1.532936	2.449603	1.803678	21	C	-3.15354	-2.40278	-0.46188
5	C	1.923232	3.617811	2.457966	22	C	-4.45586	-2.67709	-0.78894
6	C	1.461947	3.902159	3.736796	23	C	-5.52326	-1.93204	-0.20981
7	C	0.221412	0.297218	1.794251	24	C	-5.18757	-0.91055	0.718958
8	C	1.169017	-0.69698	1.453899	25	N	-6.80862	-2.18822	-0.53349
9	C	0.74101	-1.81132	0.70126	26	C	-7.88516	-1.41442	0.056824
10	O	-0.57711	-1.96715	0.415918	27	C	-7.13774	-3.24303	-1.47504
11	C	-1.48891	-1.07081	0.804131	28	N	3.85836	-3.5266	-0.09894
12	C	-1.12089	0.100874	1.482886	29	C	3.436853	-4.52758	-1.07123
13	C	-2.82974	-1.37292	0.445837	30	C	5.291708	-3.44487	0.157639
14	C	-3.88076	-0.63261	1.043391	31	C	2.998214	-5.83351	-0.42125
15	C	-3.5287	0.401044	2.074426	32	C	5.990353	-2.43746	-0.74734
16	C	-2.22412	1.100567	1.711229	33	C	2.17821	2.156658	0.478516
17	C	2.544728	-0.66059	1.777605	34	O	3.401537	2.034005	0.43943

Row	Symbol	X	Y	Z
35	N	1.401421	2.011708	-0.62107
36	C	-0.0149	2.327338	-0.68198
37	C	-0.32032	3.444858	-1.64753
38	C	-1.35832	3.313195	-2.56757
39	C	-1.6652	4.35577	-3.4402
40	C	-0.92798	5.535917	-3.4016
41	C	0.115975	5.670249	-2.48643
42	C	0.416697	4.629926	-1.61392
43	C	2.037095	1.540362	-1.84573
44	C	2.1816	0.02304	-1.80107
45	S	3.072011	-0.69017	-3.22038
46	H	0.277442	3.202504	5.396061
47	H	-0.4058	1.117253	4.256156
48	H	2.596331	4.304088	1.953086
49	H	1.764661	4.821007	4.229685
50	H	-4.33593	1.13	2.17936
51	H	-3.4221	-0.09481	3.049057
52	H	-2.38067	1.670127	0.784938
53	H	-1.94721	1.823675	2.477912
54	H	2.919713	0.149262	2.392556
55	H	4.462319	-1.50798	1.564393
56	H	1.165539	-3.58014	-0.36961
57	H	-2.35771	-2.97856	-0.92255
58	H	-4.66071	-3.46539	-1.50218
59	H	-5.96851	-0.33304	1.19903
60	H	-7.78545	-0.35037	-0.17768
61	H	-8.83395	-1.76035	-0.34504
62	H	-7.91348	-1.53319	1.144452
63	H	-8.21736	-3.29164	-1.59082
64	H	-6.69963	-3.0514	-2.45929
65	H	-6.79138	-4.21812	-1.11964
66	H	2.647202	-4.1074	-1.6995
67	H	4.283054	-4.70258	-1.74021
68	H	5.462598	-3.2203	1.212504
69	H	5.700691	-4.44612	0.002547
70	H	2.151091	-5.68309	0.253168
71	H	2.699362	-6.55729	-1.18463
72	H	3.813892	-6.27345	0.159343
73	H	5.598319	-1.4277	-0.59929
74	H	7.063933	-2.41874	-0.54017
75	H	5.854059	-2.69731	-1.80075
76	H	-0.57702	1.429188	-0.95654
77	H	-0.33729	2.617405	0.318267
78	H	-1.92973	2.388675	-2.60539
79	H	-2.47549	4.241774	-4.15492
80	H	-1.16168	6.347904	-4.08445
81	H	0.695996	6.588377	-2.45347
82	H	1.235044	4.735712	-0.90625
83	H	1.418755	1.854395	-2.68898
84	H	3.01361	2.014527	-1.95191
85	H	2.779016	-0.26088	-0.93405
86	H	1.208134	-0.4617	-1.70869
87	H	2.150219	-0.39779	-4.16308

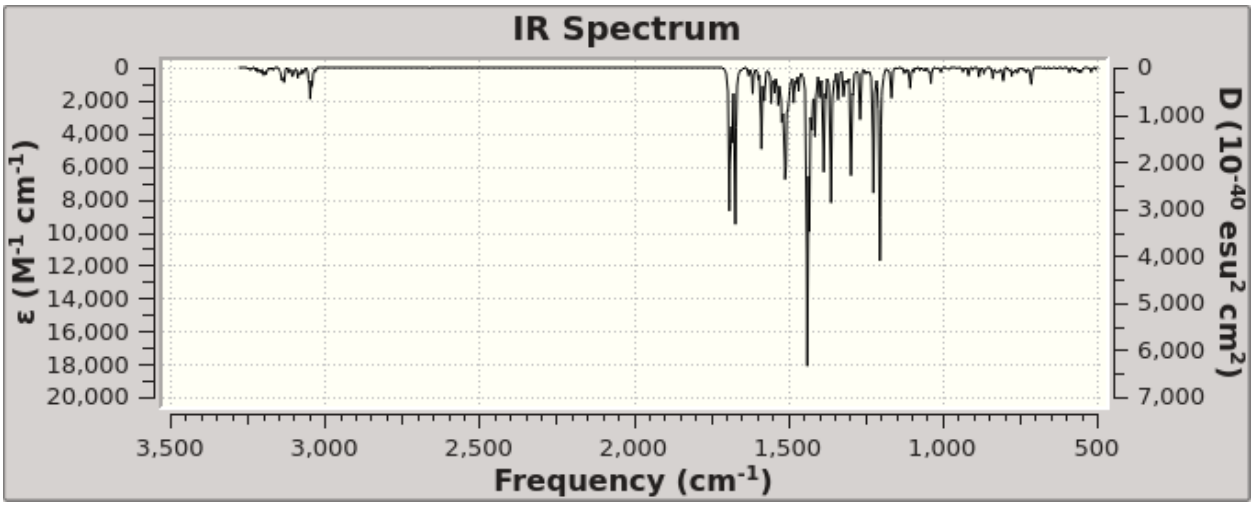

Figure S6. Calculated IR spectrum for probe **B**.

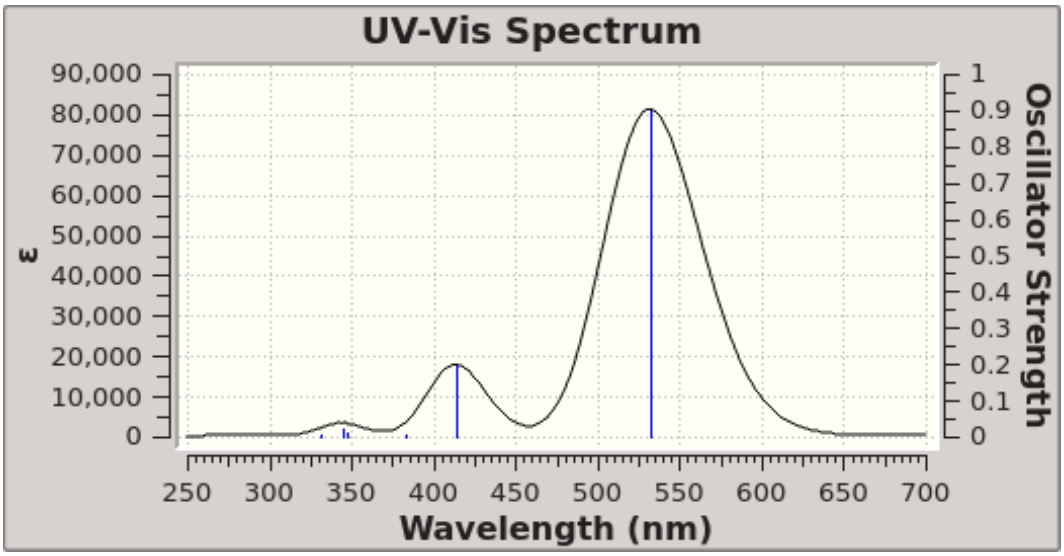

Figure S7. Calculated UV-Vis spectrum for probe **B**.

Table S4. Excitation energies and oscillator strengths listing for probe **B**.

Excited State	**Nature**	**E (eV)**	**λ (nm)**	***f***	**Orbital transitions**	**Normalized coefficient**
1:	A	2.3304	532.03	0.9011	164 -> 165	0.70160
2:	A	2.9961	413.82	0.1955	163 -> 165	0.68669
3:	A	3.2334	383.45	0.0030	162 -> 165	0.69886
4:	A	3.5665	347.64	0.0117	160 -> 165	0.33730
					161 -> 165	0.59831
5:	A	3.5996	344.44	0.0203	156 -> 165	-0.12737
					159 -> 165	-0.13730
					160 -> 165	0.59072
					161 -> 165	-0.33178
6:	A	3.7415	331.38	0.0056	156 -> 165	-0.11208
					157 -> 165	-0.20537
					158 -> 165	0.60391
					164 -> 166	0.23510

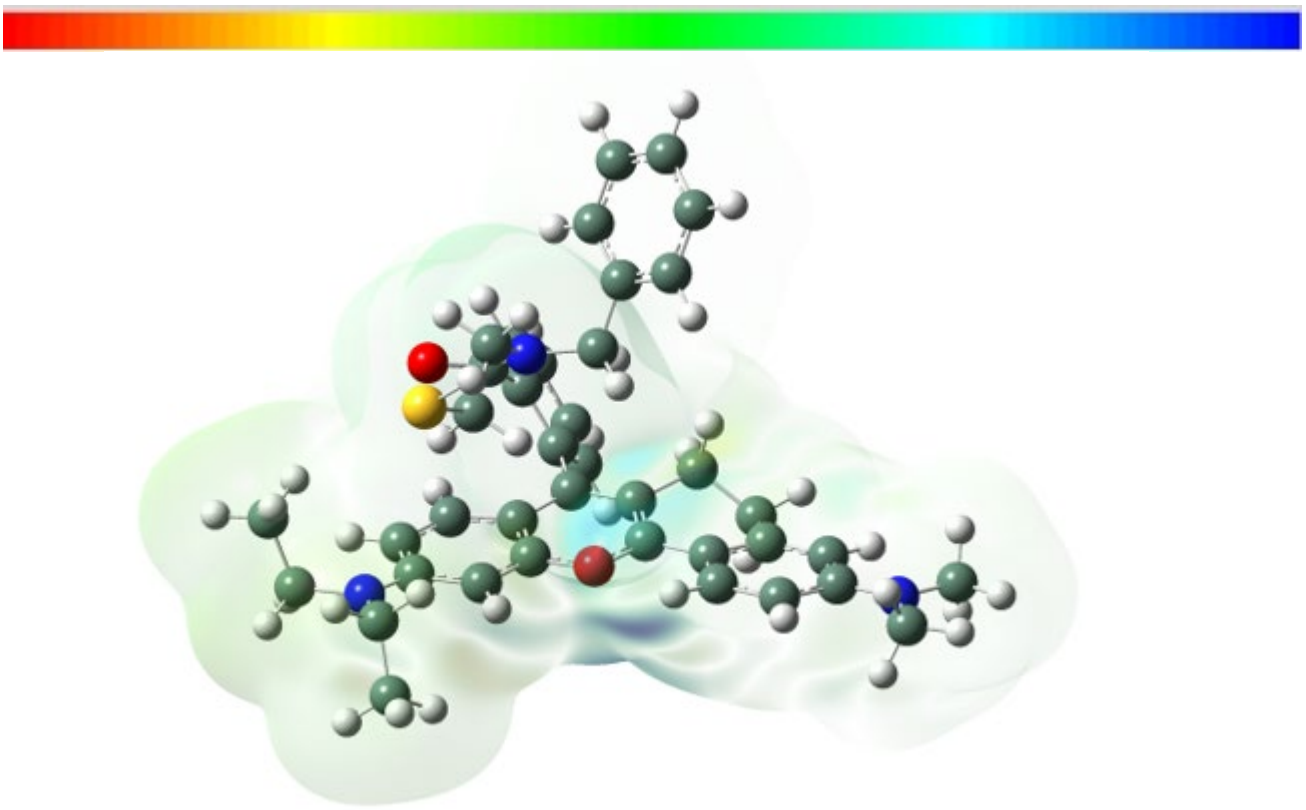

Figure 8. Current density difference illustrations as iso-surfaces of **B**, as indicated for excited state (ES 1, see Table S4). Red areas indicate values for the different density of $-1.552e^{-4}$ and blue are for $1.552e^{-4}$, see chart on top of the illustration.

Data for C.

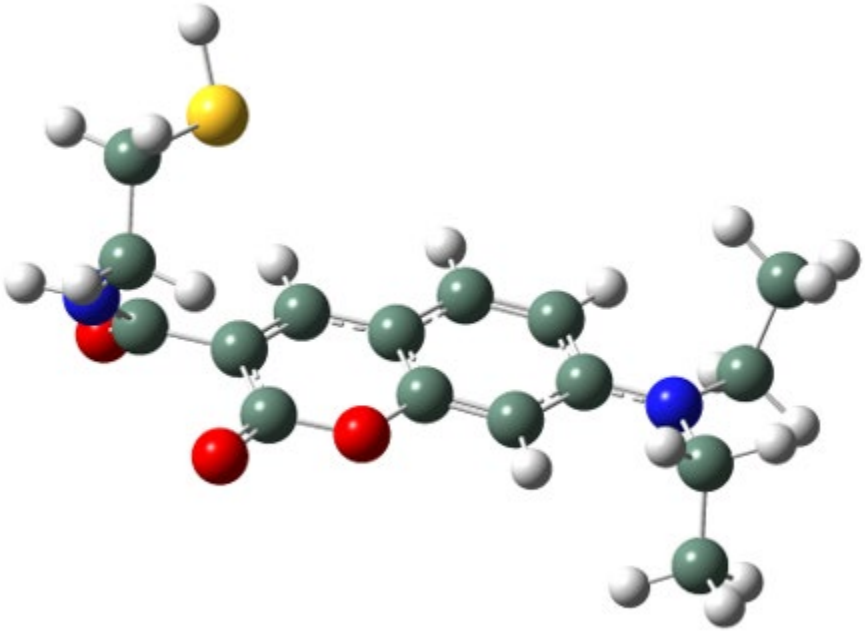

Figure S9. GaussView representation of 7-(diethylamino)-N-(2-mercaptoethyl)-2-oxo-2H-chromene-3-carboxamide, **C**.

Table S5. Calculated atomic coordinates for probe **C**.

Row	Symbol	X	Y	Z
1	S	3.408661	2.224012	-0.87622
2	C	4.611519	1.057013	-1.62033
3	C	4.264381	-0.37488	-1.23188
4	N	4.424109	-0.63583	0.184108
5	C	3.476992	-0.58223	1.146396
6	O	3.773011	-0.50276	2.339022
7	C	2.043229	-0.61486	0.735358
8	C	1.531369	-1.68919	-0.08317
9	O	0.177823	-1.66488	-0.36962
10	C	-0.66548	-0.70034	0.092123
11	C	-0.18293	0.323128	0.930087
12	C	1.190271	0.323751	1.245496
13	C	-1.98711	-0.79293	-0.2854
14	C	-2.91977	0.167436	0.169441
15	C	-2.43781	1.210468	1.018796
16	C	-1.11752	1.276402	1.380504
17	O	2.163484	-2.62215	-0.53426
18	N	-4.22564	0.103344	-0.1881
19	C	-5.22596	1.011146	0.35768
20	C	-4.71478	-0.88865	-1.13525
21	C	-5.09599	-2.20674	-0.47171
22	C	-5.35856	2.301062	-0.44252
23	H	4.582309	1.149563	-2.70856
24	H	5.617787	1.313138	-1.2798
25	H	3.245859	-0.61647	-1.53065
26	H	4.918751	-1.05602	-1.78324
27	H	5.368393	-0.59679	0.545463
28	H	1.585639	1.098939	1.896735
29	H	-2.27969	-1.6248	-0.91256
30	H	-3.11251	1.978013	1.375118
31	H	-0.77493	2.08387	2.021631
32	H	-6.17735	0.47247	0.366158
33	H	-4.99822	1.216692	1.406166
34	H	-5.58255	-0.45404	-1.63868
35	H	-3.96751	-1.04046	-1.9182
36	H	-5.88446	-2.05612	0.271241
37	H	-5.46686	-2.91712	-1.21612
38	H	-4.24147	-2.66242	0.035437
39	H	-5.63647	2.091219	-1.4794
40	H	-6.1325	2.941975	-0.01039

Row	Symbol	X	Y	Z
41	H	-4.42079	2.862851	-0.45486
42	H	4.042975	3.353521	-1.25284

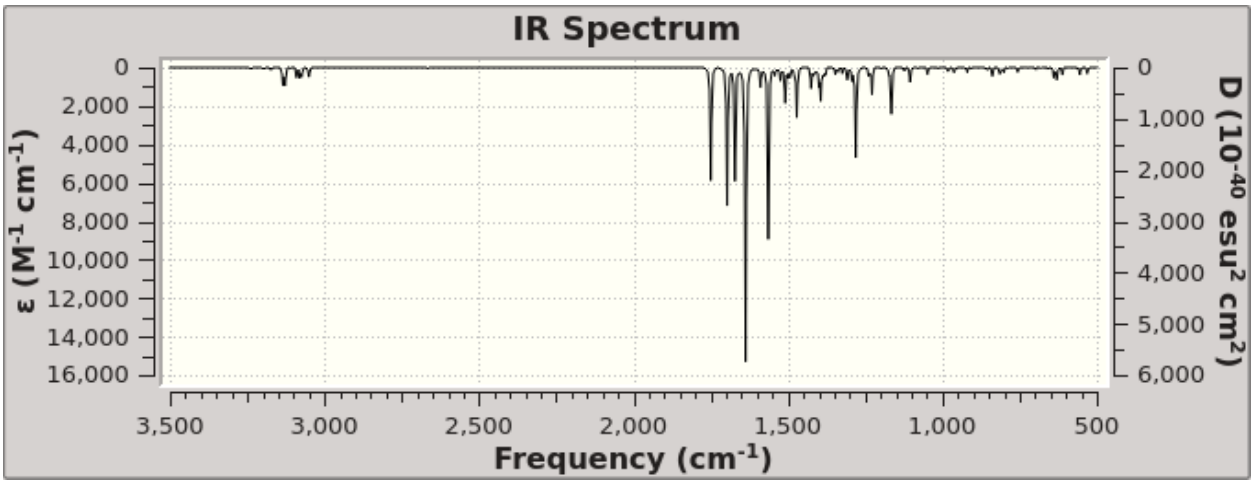

Figure S10. Calculated IR spectrum for Probe **C**.

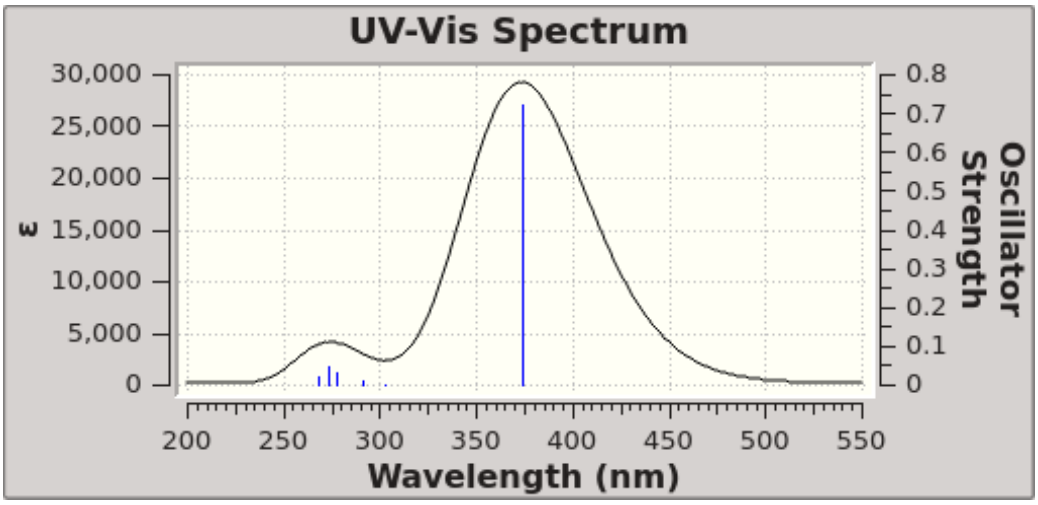

Figure S11. Calculated UV-Vis spectrum for probe **C**.

Table S6. Excitation energies and oscillator strengths listing for probe **C**.

Excited State	Nature	E (eV)	λ(nm)	*f*	Orbital transitions	Normalized coefficient
1:	A	3.3182	373.65	0.7191	85 -> 86	0.70046
2:	A	4.0987	302.50	0.0017	84 -> 86	0.70498
3:	A	4.2561	291.31	0.0079	83 -> 86	0.55577
					85 -> 87	-0.38747
					85 -> 88	0.14053
4:	A	4.4624	277.84	0.0295	80 -> 86	0.12760
					81 -> 86	-0.24294
					82 -> 86	0.38036
					83 -> 86	0.34045
					85 -> 87	0.38640
5:	A	4.5443	272.84	0.0464	82 -> 86	0.54729
					83 -> 86	-0.22418
					85 -> 87	-0.35543
6:	A	4.6306	267.75	0.0198	79 -> 86	0.11731
					80 -> 86	-0.24039
					81 -> 86	0.56418
					82 -> 86	0.18408
					83 -> 86	0.10310
					85 -> 87	0.17768
					85 -> 88	-0.14201

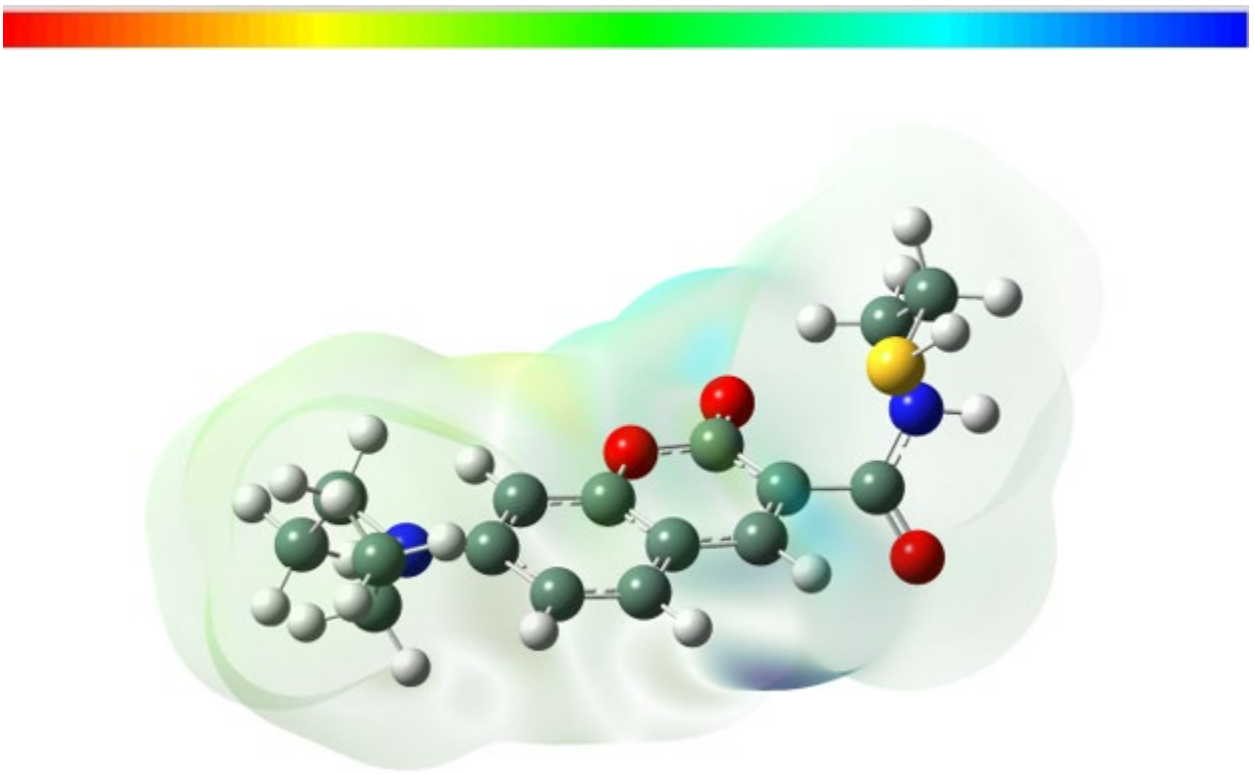

Figure S12. Current density difference illustrations as iso-surfaces of **C**, as indicated for excited state (ES 1, see Table S4). Red areas indicate values for the different density of $-1.667e^{-4}$ and blue are for $1.667e^{-4}$, see chart on top of the illustration

5. Kinetic test of probe **A** with different concentrations of DTT, Cys and Hcy.

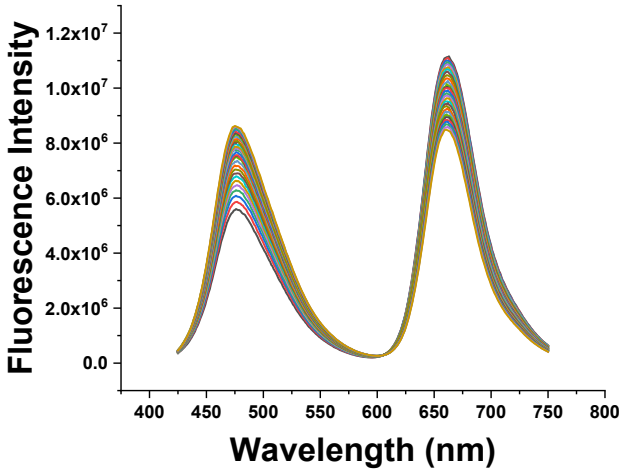

Figure S13. Fluorescence spectra of time dependent (30 min) test of 5 μM probe **A** with 100 μM DTT under excitation at 405 nm.

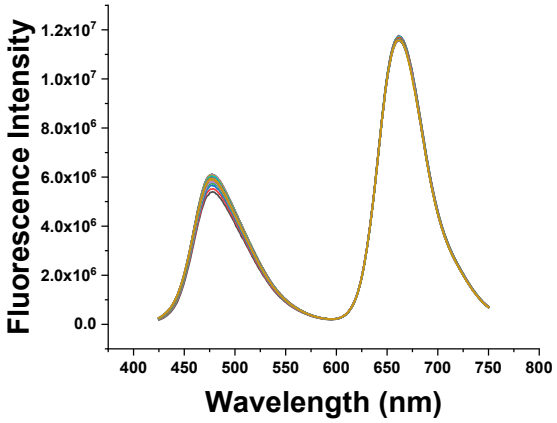

Figure S14. Fluorescence spectra of time dependent (30 min) test of 5 μM probe **A** with 100 μM Cys under excitation at 405 nm.

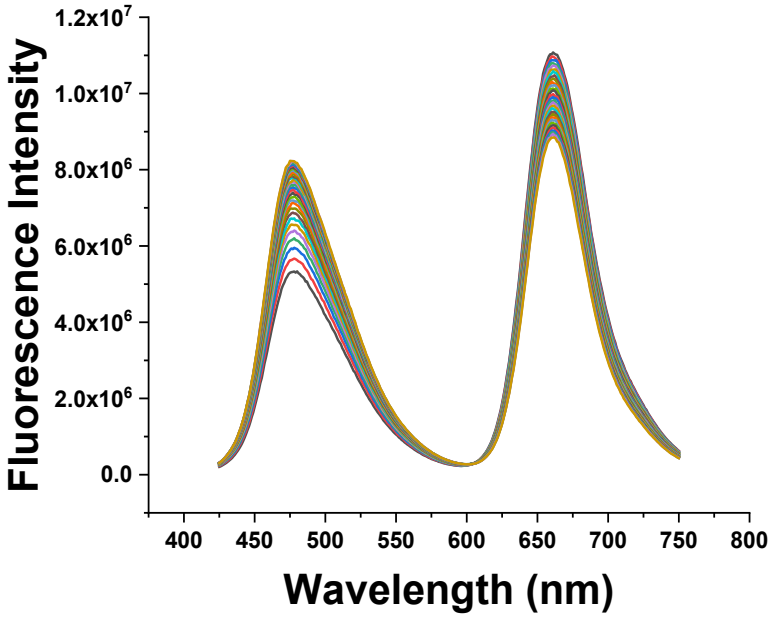

Figure S15. Fluorescence spectra of time dependent (30 min) test of 5 μM probe **A** with 500 μM Cys under excitation at 405 nm.

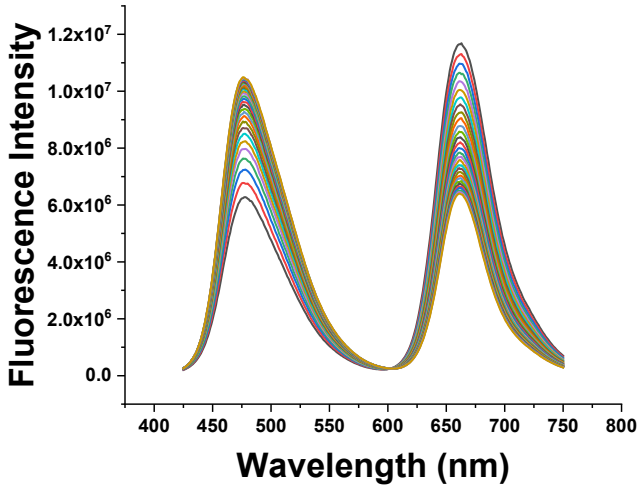

Figure S16. Fluorescence spectra of time dependent (30 min) test of 5 μM probe **A** with 1000 μM Cys under excitation at 405 nm.

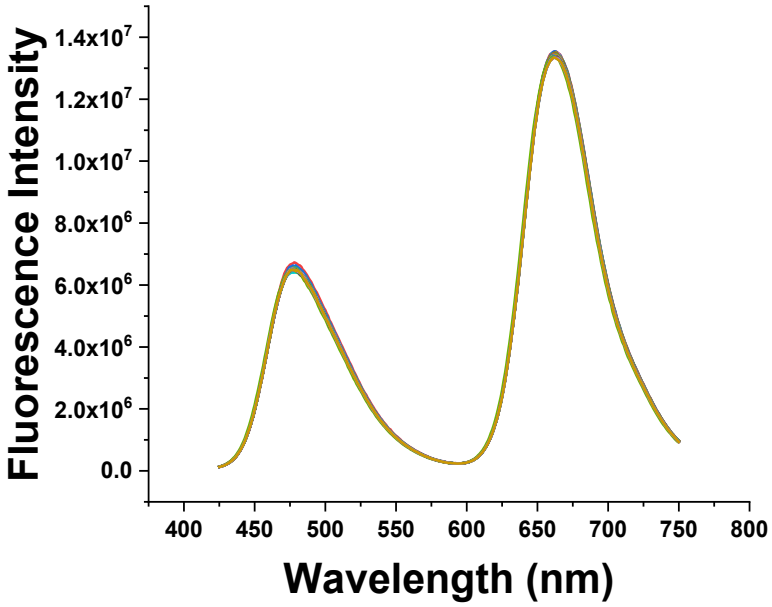

Figure S17. Fluorescence spectra of time dependent (30 min) test of 5 μM probe **A** with 100 μM Hcy under excitation at 405 nm.

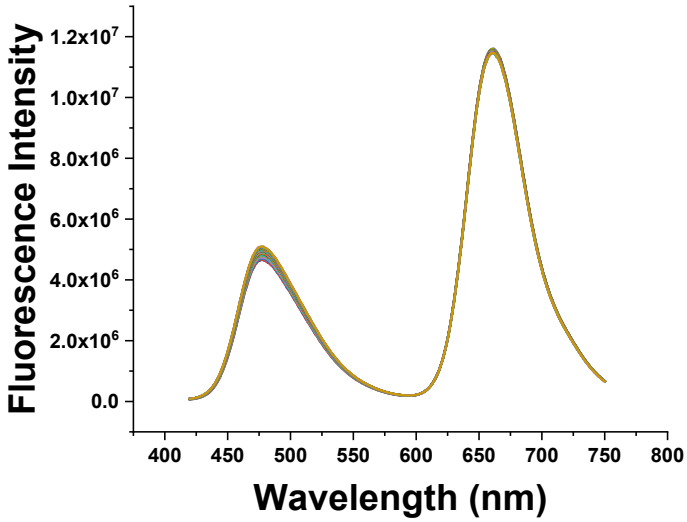

Figure S18. Fluorescence spectra of time dependent (30 min) test of 5 μM probe **A** with 500 μM Hcy under excitation at 405 nm.

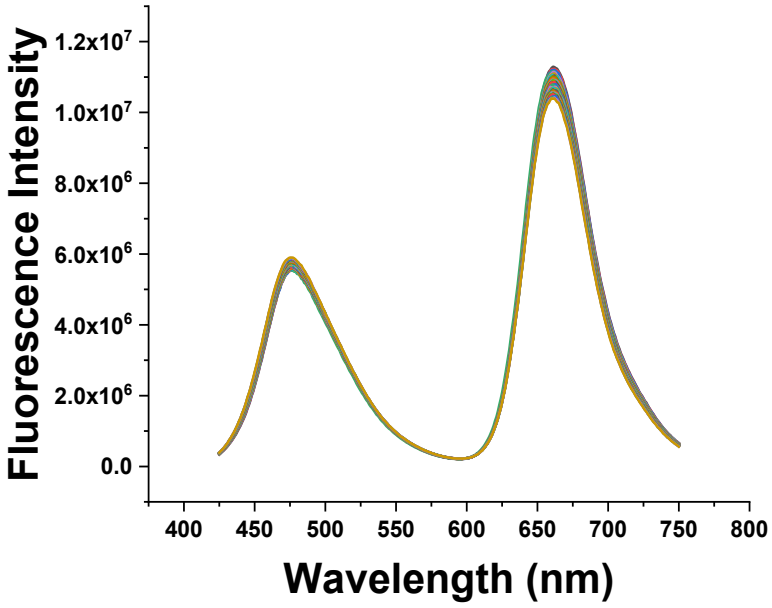

Figure S19. Fluorescence spectra of time dependent (30 min) test of 5 μM probe **A** with 1000 μM Hcy under excitation at 405 nm.

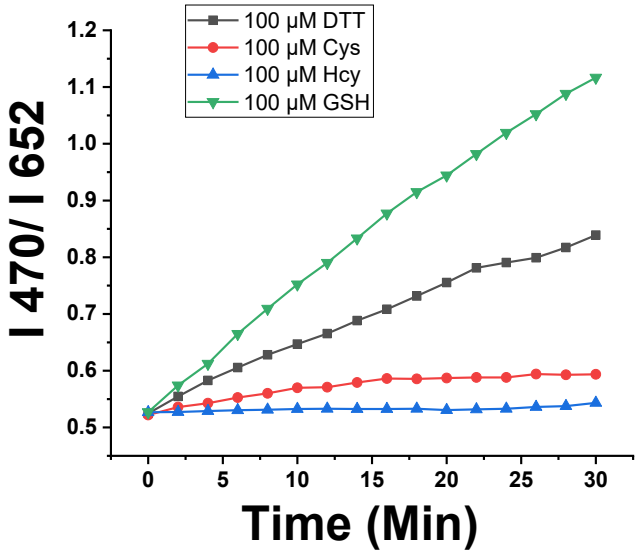

Figure S20. Fluorescence wavelength ratiometric plot of 5 μM probe **A** with 100 μM different biothiols or DTT for 30 min, constructed by taking the fluorescence intensity at 470 nm divided by the fluorescence intensity at 652 nm under excitation at 405 nm.

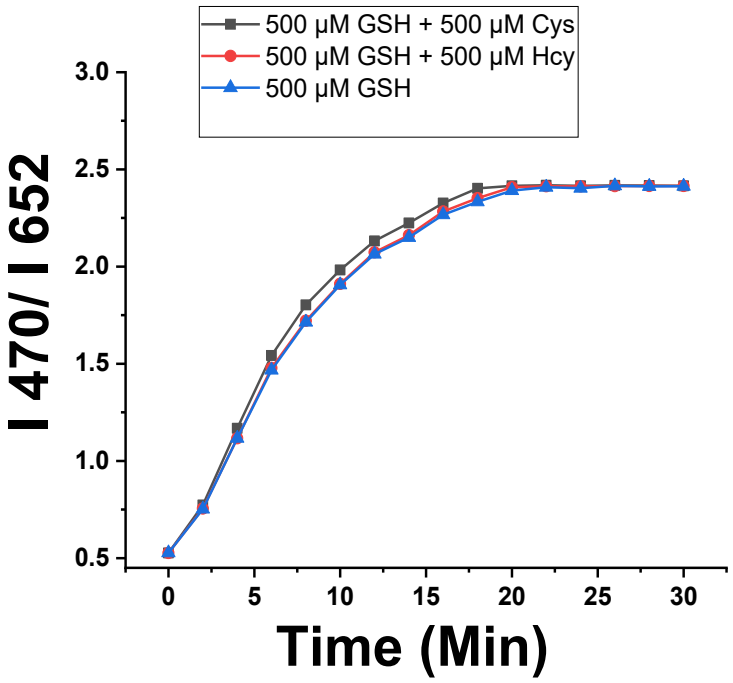

Figure S21. Fluorescence wavelength ratiometric plot of 5 μM probe **A** with 500 μM GSH, 500 μM GSH with 500 μM Cys or 500 μM GSH with 500 μM Hcy for 30 min, constructed by taking the fluorescence intensity at 470 nm divided by the fluorescence intensity at 652 nm under excitation at 405 nm.

6. Photostability of probe A

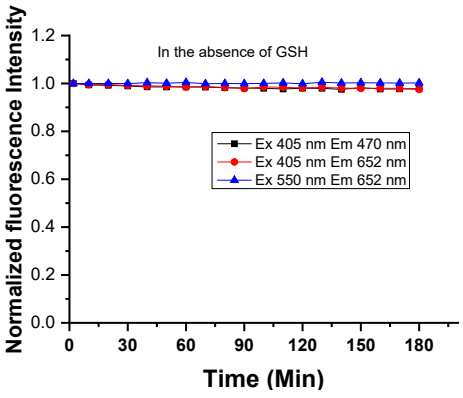

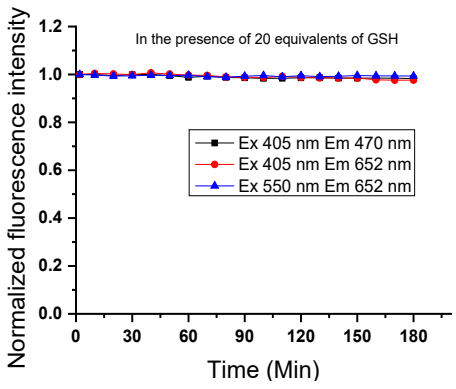

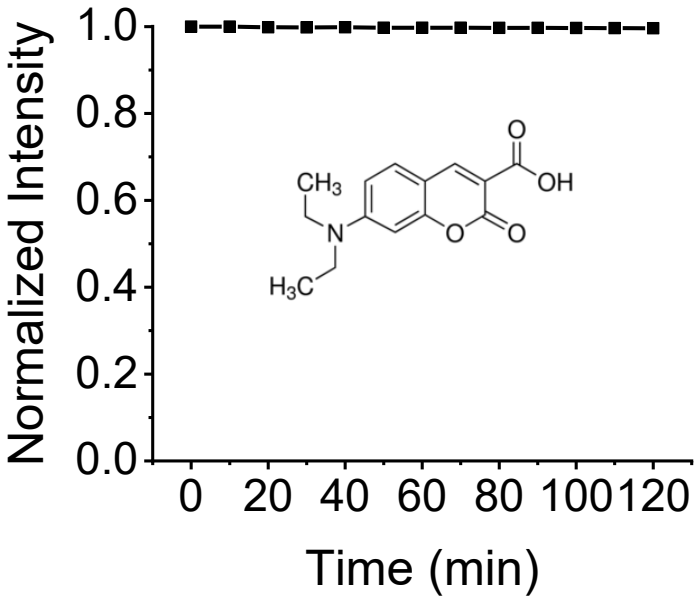

Figure S22. Coumarin and rhodamine fluorescence intensity of 5 μM probe **A** in the absence (upper, left) and presence (upper, right) of 20 equivalents of GSH in a 20 mM PBS buffer (pH 7.4) containing 30% ethanol under 180-minute excitation at 405 nm or 550 nm. Fluorescence intensity (lower) of 7-(diethylamino)coumarin-3-carboxylic acid in 20 mM PBS buffer (pH 7.4) containging 30% ethanol ethanol under 180-minute excitation at 405 nm. Slit: excitation/emission = 5.0/10.0 nm

7. Ratiometric image of HeLa cells

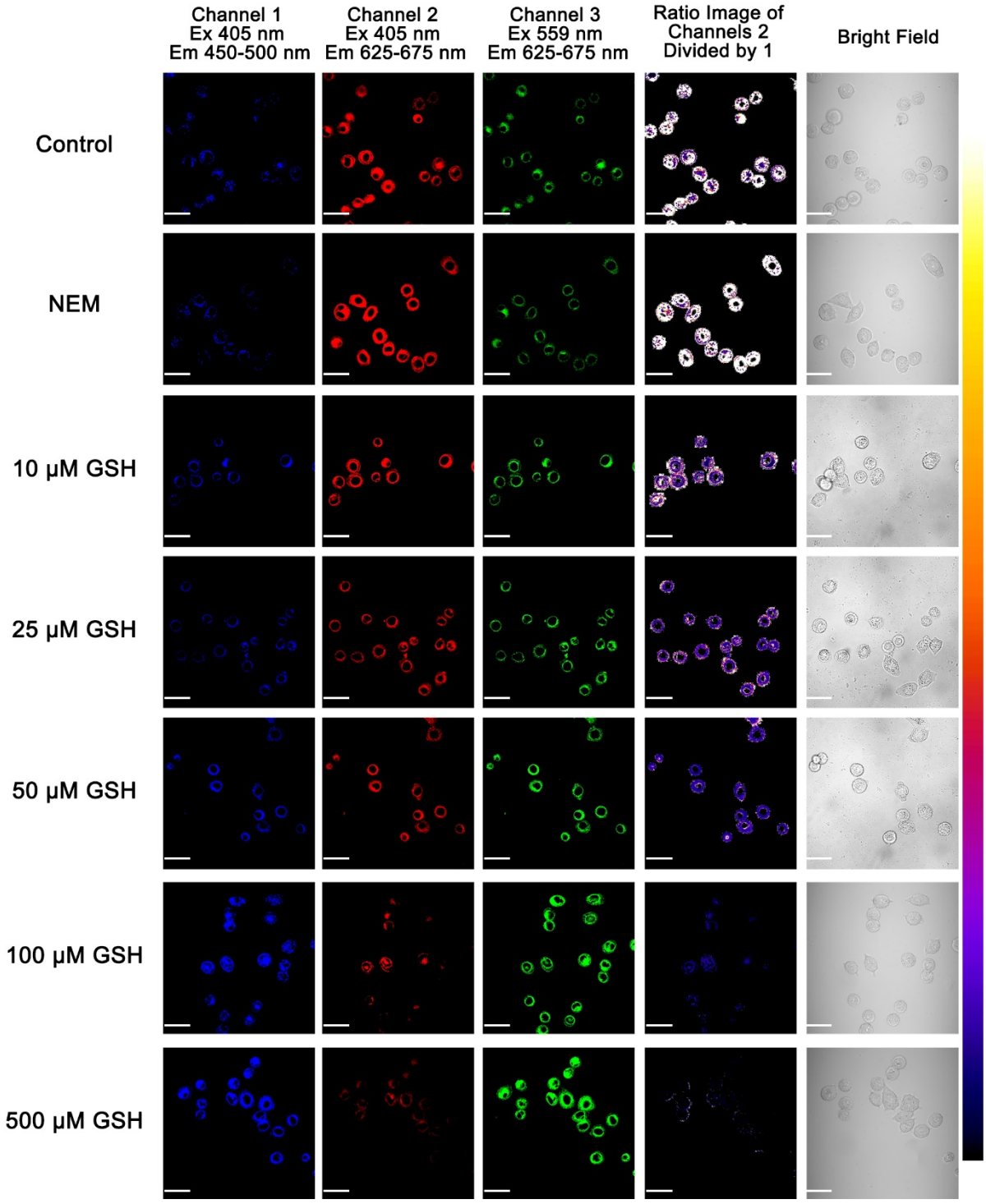

Figure S23. Ratiometric cellular fluorescence images of HeLa cells incubated with 10 μM probe **A** before and after NEM treatment or external GSH incubation. Scale bar: 50 μM.

Ratiometric image of Drosophila melanogaster larvae

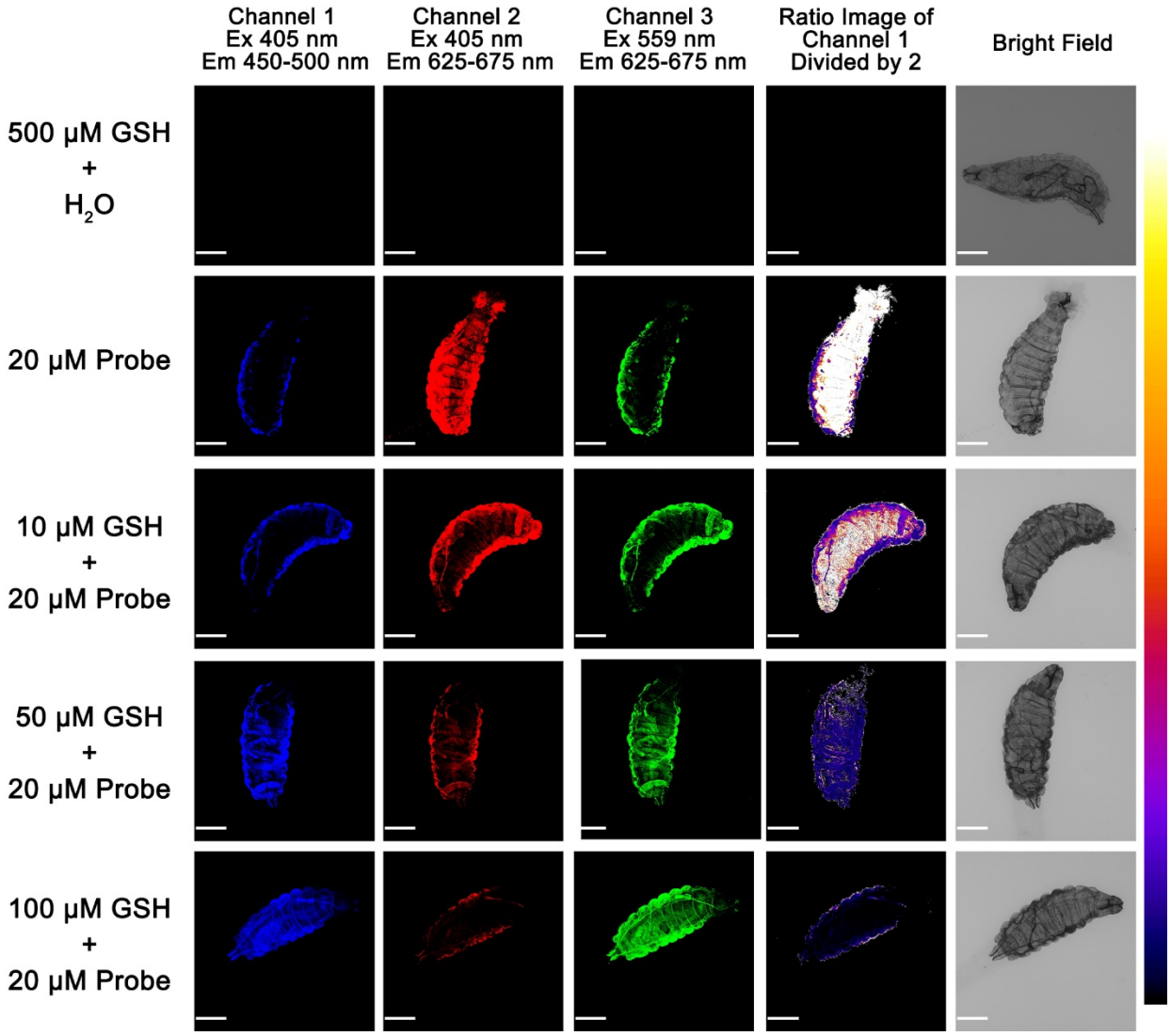

Figure S24. Ratiometric fluorescence images of *Drosophila melanogaster* larvae incubated with 10 μM probe **A** before and after further external GSH incubation. Scale bar: 100 μM

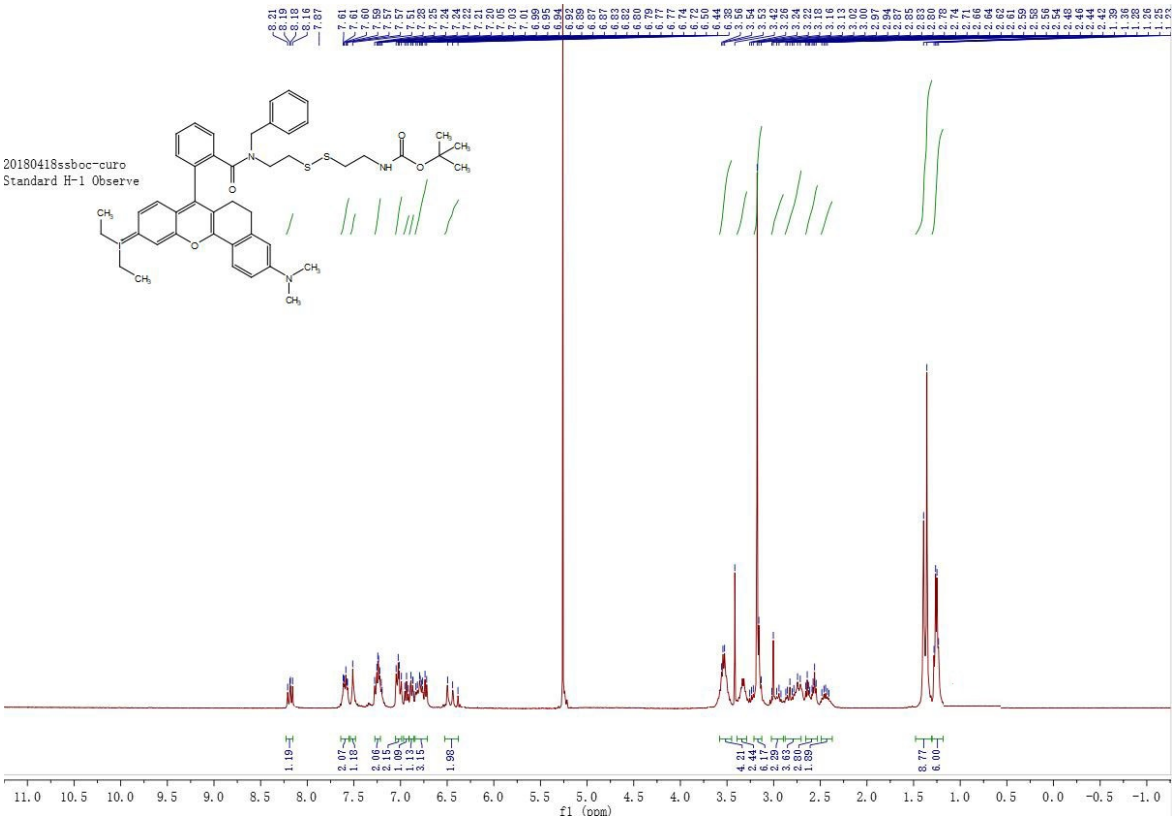

Figure S25. ^{1}H NMR and $^{13}CNMR$ of compound 6 in $CDCl_3$ solution.

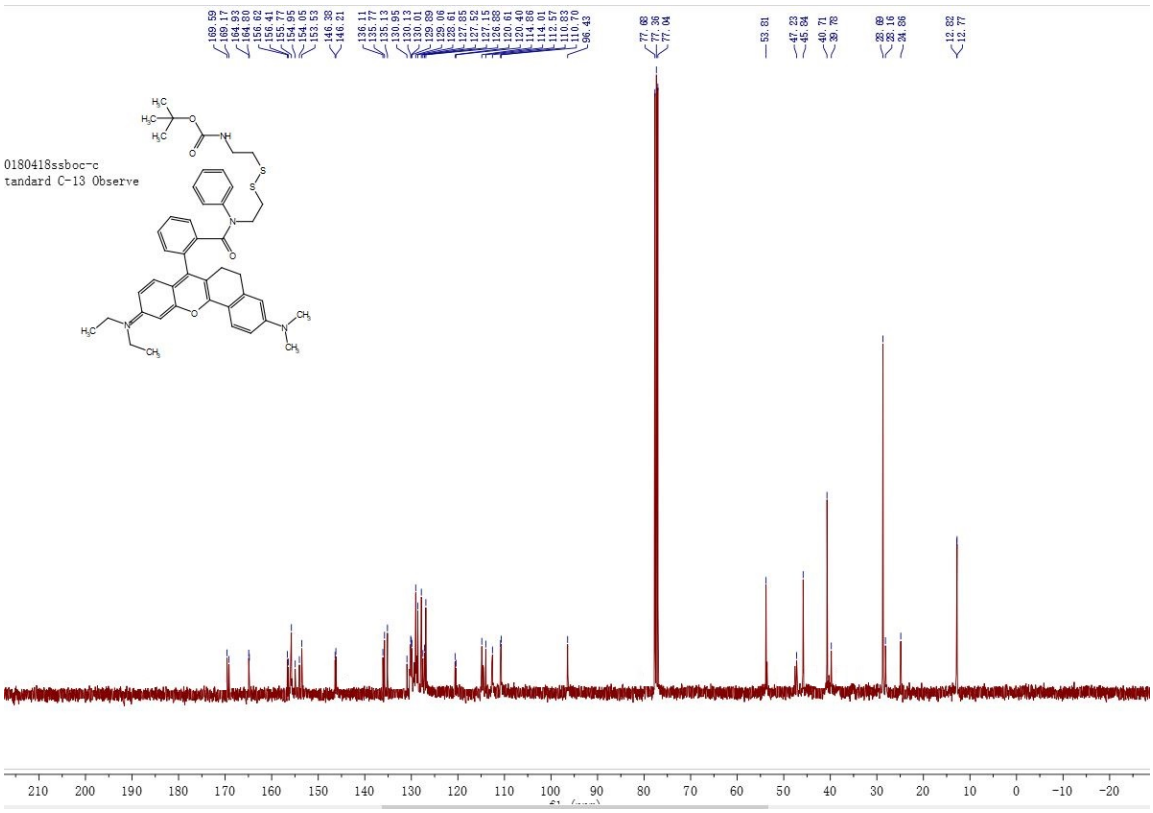

Figure S26. ^{13}C NMR spectrum of compound **6** in $CDCl_3$ solution.

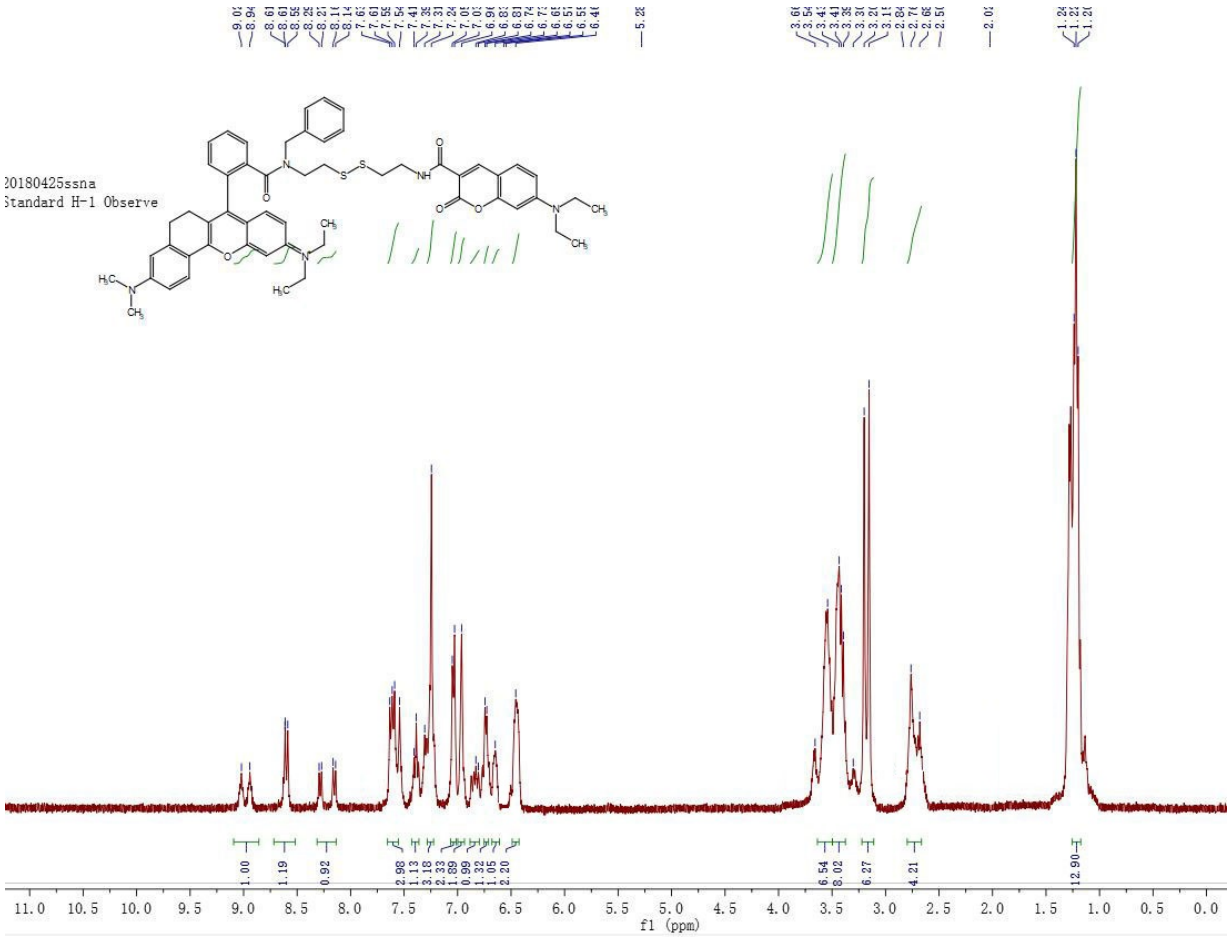

Figure S27. ^{1}HNMR spectrum of probe **A** in $CDCl_3$ solution.

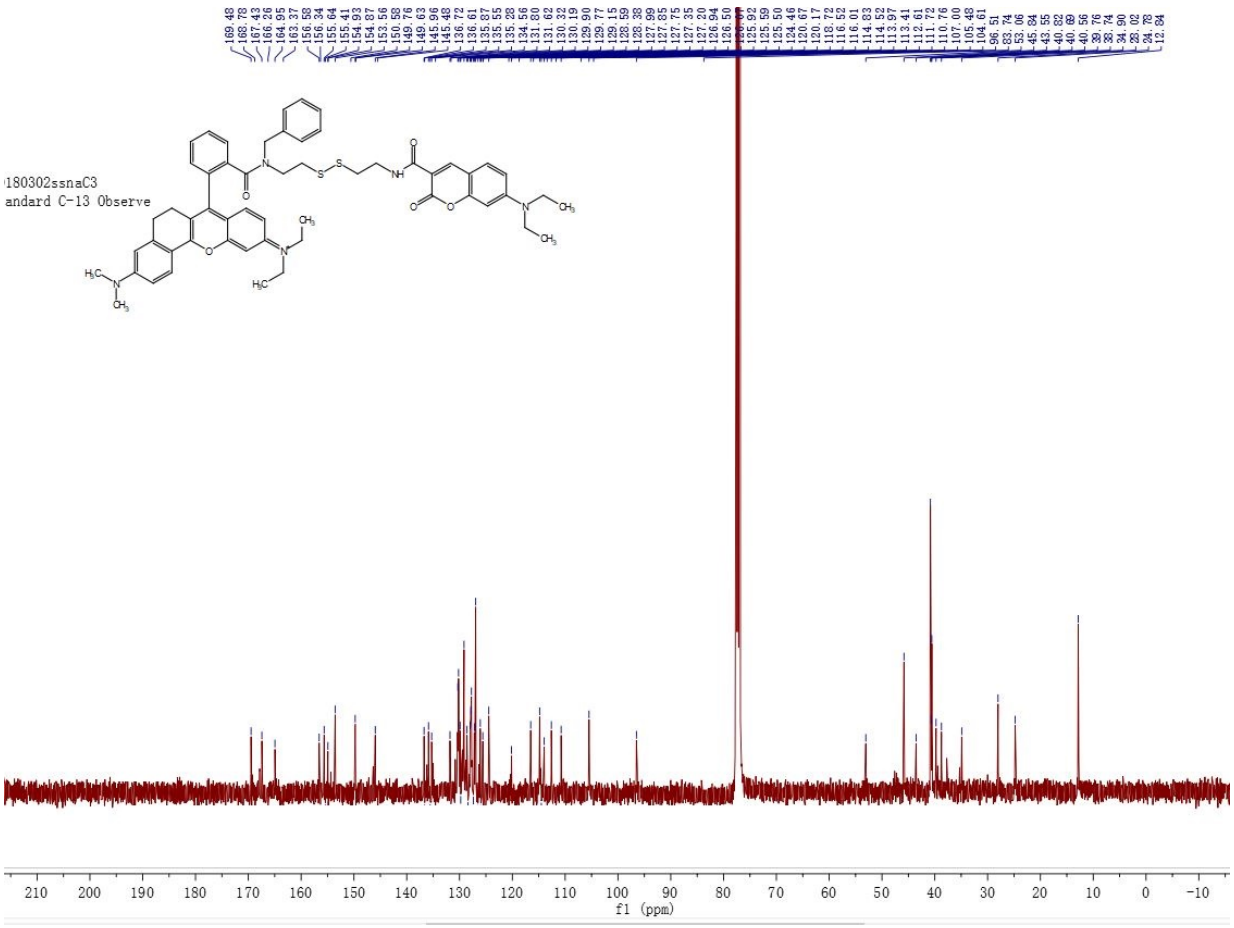

Figure S28. ^{1}HNMR spectrum of probe **A** in $CDCl_3$ solution.

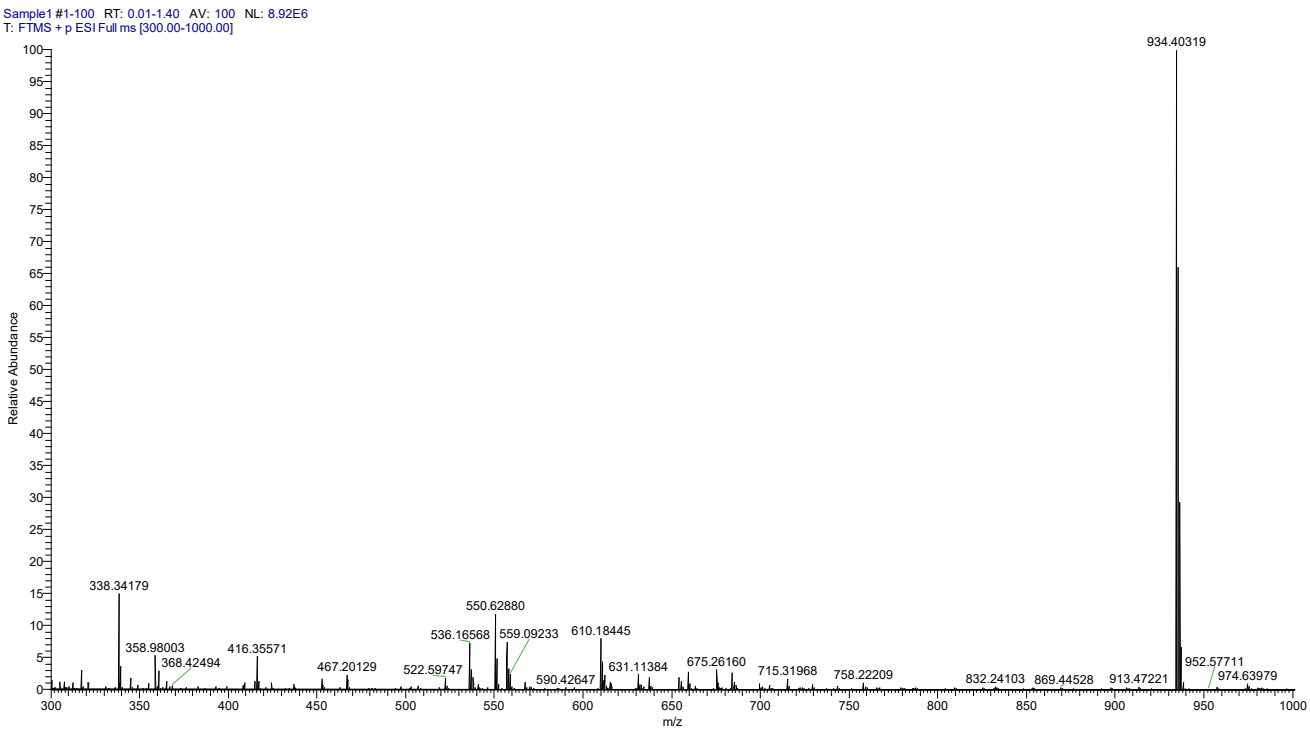

Figure S29. HR-MS spectrum of probe **A**.

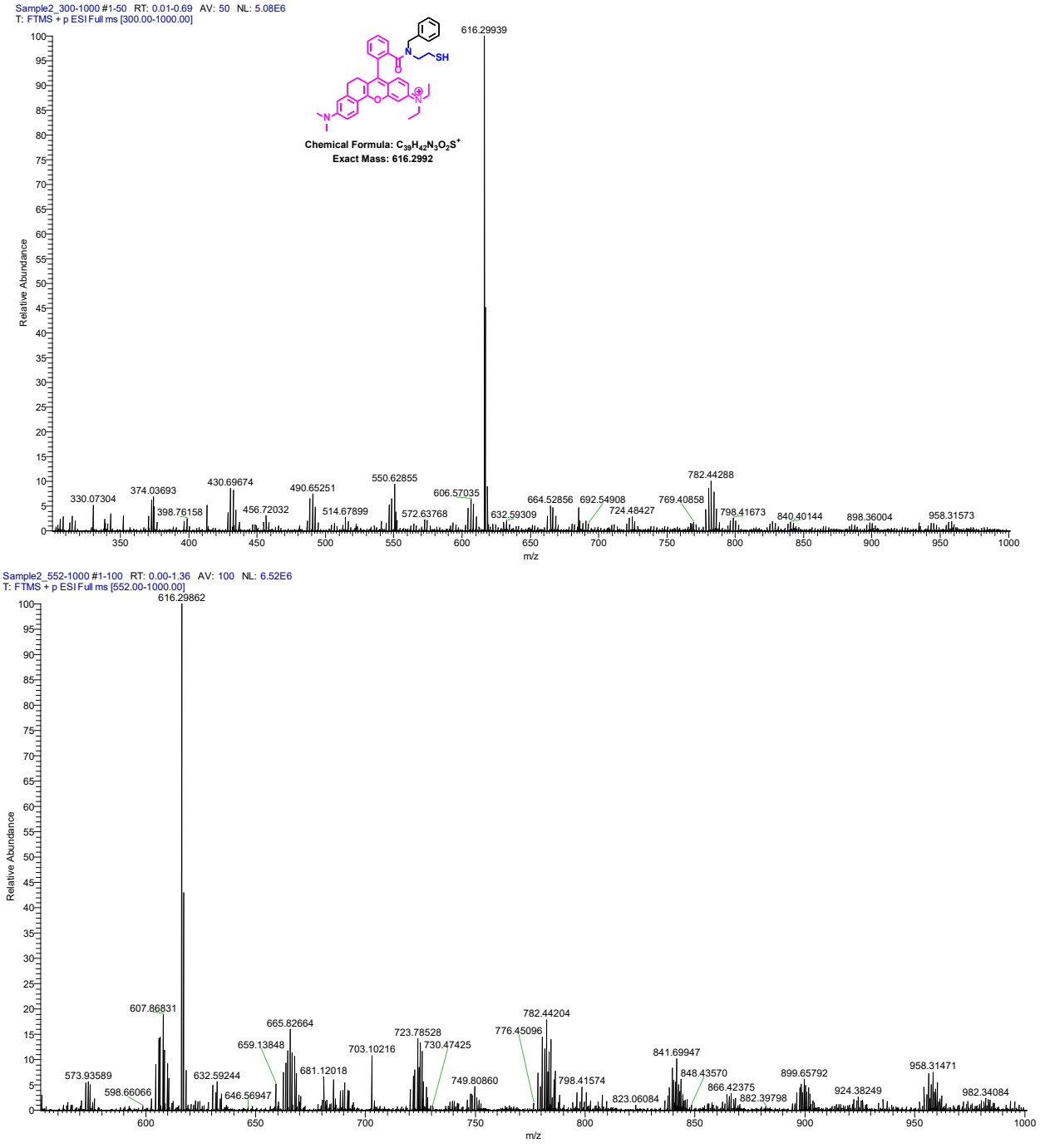

Figure S30. HR-MS spectrums of probe **A** reactions with DTT (top) and GSH (bottom).

8. References

(1) Zhang, Y. S.; Zhang, J. Q.; Su, M. H.; Li, C. H. Rational molecular design of a reversible BODIPY-Based fluorescent probe for real-time imaging of GSH dynamics in living cells. *Biosens. Bioelectron.* **2021,** *175*, DOI: 10.1016/j.bios.2020.112866.
(2) Zhang, H.; Yue, X. X.; Li, W. X.; Chen, W. Q.; Wang, Y. G.; Li, X.; Ye, Y.; Song, X. Z. Selective and discriminative fluorescence sensing of Cys, Hcy, GSH and H2S with concise and distinct signals. *Sens. Actuator B-Chem.* **2021,** *331*, DOI: 10.1016/j.snb.2020.129394.
(3) Yue, X. X.; Chen, J. L.; Chen, W. Q.; Wang, B. H.; Zhang, H.; Song, X. Z. An endoplasmic reticulum-targeting fluorescent probe for discriminatory detection of Cys, Hcy and GSH in living cells. *Spectrochimica Acta Part a-Molecular and Biomolecular Spectroscopy* **2021,** *250*, DOI: 10.1016/j.saa.2020.119347.
(4) Yang, Y. Z.; Xu, Z. Y.; Han, L.; Fan, Y. Z.; Qing, M.; Li, N. B.; Luo, H. Q. A simple fluorescent probe with two different fluorescence signals for rapid sequence distinguishing of Cys/Hcy/GSH and intracellular imaging. *Dyes Pigment.* **2021,** *184*, DOI: 10.1016/j.dyepig.2020.108722.
(5) Yang, Y.; Feng, Y.; Li, H.; Shen, R.; Wang, Y. Z.; Song, X. R.; Cao, C.; Zhang, G. L.; Liu, W. S. Hydro-soluble NIR fluorescent probe with multiple sites and multiple excitations for distinguishing visualization of endogenous Cys/Hcy, and GSH. *Sens. Actuator B-Chem.* **2021,** *333*, DOI: 10.1016/j.snb.2020.129189.
(6) Luo, W. F.; Zhang, S.; Meng, Q. H.; Zhou, J.; Jin, R. Y.; Long, X.; Tang, Y. P.; Guo, H. A two-photon multi-emissive fluorescent probe for discrimination of Cys and Hcy/GSH via an aromatic substitution-rearrangement. *Talanta* **2021,** *224*, DOI: 10.1016/j.talanta.2020.121833.
(7) Zhu, L. L.; Zhang, T. G.; Ma, Y. Y.; Lin, W. Y. Discriminating Cys from GSH/H2S in vitro and in vivo with a NIR fluorescent probe. *Sens. Actuator B-Chem.* **2020,** *305*, DOI: 10.1016/j.snb.2019.127202.
(8) Ren, X. J.; Zhang, Y.; Zhang, F.; Zhong, H.; Wang, J. P.; Liu, X. J.; Yang, Z. G.; Song, X. Z. Red-emitting fluorescent probe for discrimination of Cys/Hcy and GSH with a large Stokes shift under a single-wavelength excitation. *Anal. Chim. Acta* **2020,** *1097*, 245-253, DOI: 10.1016/j.aca.2019.11.030.
(9) Li, R. X.; Kassaye, H.; Pan, Y. P.; Shen, Y. Z.; Li, W. Q.; Cheng, Y. R.; Guo, J. X.; Xu, Y.; Yin, H. P.; Yuan, Z. W. A visible and near-infrared dual-fluorescent probe for discrimination between Cys/Hcy and GSH and its application in bioimaging. *Biomaterials Science* **2020,** *8* (21), 5994-6003, DOI: 10.1039/d0bm01237h.
(10) Jia, L.; Niu, L. Y.; Yang, Q. Z. Fluorescent Probe for Simultaneous Discrimination of GSH, Cys, and SO2 Derivatives. *Anal. Chem.* **2020,** *92* (15), 10800-10806, DOI: 10.1021/acs.analchem.0c02255.
(11) Wang, L.; Wang, J. B.; Xia, S.; Wang, X. X.; Yu, Y. T.; Zhou, H. W.; Liu, H. Y. A FRET-based near-infrared ratiometric fluorescent probe for detection of mitochondria biothiol. *Talanta* **2020,** *219*, DOI: 10.1016/j.talanta.2020.121296.
(12) Xia, S.; Zhang, Y. B.; Fang, M. X.; Mikesell, L.; Steenwinkel, T. E.; Wan, S. L.; Phillips, T.; Luck, R. L.; Werner, T.; Liu, H. Y. A FRET-Based Near-Infrared Fluorescent Probe for Ratiometric Detection of Cysteine in Mitochondria. *Chembiochem* **2019,** *20* (15), 1986-1994, DOI: 10.1002/cbic.201900071.

(13) Yuan, L.; Lin, W.; Yang, Y.; Chen, H. A Unique Class of Near-Infrared Functional Fluorescent Dyes with Carboxylic-Acid-Modulated Fluorescence ON/OFF Switching: Rational Design, Synthesis, Optical Properties, Theoretical Calculations, and Applications for Fluorescence Imaging in Living Animals. *Journal of the American Chemical Society* **2012,** *134* (2), 1200-1211, DOI: 10.1021/ja209292b.
(14) Zhang, Y.; Xia, S.; Fang, M.; Mazi, W.; Zeng, Y.; Johnston, T.; Pap, A.; Luck, R. L.; Liu, H. New near-infrared rhodamine dyes with large Stokes shifts for sensitive sensing of intracellular pH changes and fluctuations. *Chemical Communications* **2018,** *54* (55), 7625-7628, DOI: 10.1039/C8CC03520B.
(15) Brouwer, A. M. Standards for photoluminescence quantum yield measurements in solution (IUPAC Technical Report). *Pure and Applied Chemistry* **2011,** *83* (12), 2213-2228, DOI: 10.1351/pac-rep-10-09-31.
(16) Gong, Y.-J.; Zhang, X.-B.; Mao, G.-J.; Su, L.; Meng, H.-M.; Tan, W.; Feng, S.; Zhang, G. A unique approach toward near-infrared fluorescent probes for bioimaging with remarkably enhanced contrast. *Chemical Science* **2016,** *7* (3), 2275-2285, DOI: 10.1039/C5SC04014K.
(17) Rojas-Chapana, J.; Troszczynska, J.; Firkowska, I.; Morsczeck, C.; Giersig, M. Multi-walled carbon nanotubes for plasmid delivery into Escherichia coli cells. *Lab on a Chip* **2005,** *5* (5), 536-539.